Clear cell squamous cell carcinoma of the tongue exhibits characteristics as an undifferentiated squamous cell carcinoma

Hasegawa, Kana
Laboratory of Oral Pathology, Division of Maxillofacial Diagnostic and Surgical Sciences, Faculty of Dental Science, Kyushu University

Fujii, Shinsuke
Laboratory of Oral Pathology, Division of Maxillofacial Diagnostic and Surgical Sciences, Faculty of Dental Science, Kyushu University

Kurppa, Kari J.
Institute of Biomedicine and MediCity Research Laboratories, University of Turku

Maehara, Takashi
Dento-craniofacial Development and Regeneration Research Center, Division of Maxillofacial Diagnostic and Surgical Sciences, Faculty of Dental Science, Kyushu University

他

出版情報：Pathology - Research and Practice. 235, pp.153909-, 2022-07. Elsevier
バージョン：

Clear cell squamous cell carcinoma of the tongue exhibits characteristics as an undifferentiated squamous cell carcinoma

Kana Hasegawa[1,5], Shinsuke Fujii[1,2,5], Kari J Kurppa[3], Takashi Maehara[2,4], Kazunari Oobu[4], Seiji Nakamura[4] and Tamotsu Kiyoshima[1,*]

[1]Laboratory of Oral Pathology, [2]Dento-craniofacial Development and Regeneration Research Center, and [4]Section of Maxillofacial Oncology, Division of Maxillofacial Diagnostic and Surgical Sciences, Faculty of Dental Science, Kyushu University, 3-1-1 Maidashi, Higashi-ku, Fukuoka 812-8582, Japan.

[3]Institute of Biomedicine and MediCity Research Laboratories, University of Turku, and Turku Bioscience Centre, University of Turku and Åbo Akademi University, Turku, FI-20520, Finland

[5]These authors contributed equally to this work.

*Corresponding author: Laboratory of Oral Pathology, Division of Maxillofacial Diagnostic and Surgical Sciences, Faculty of Dental Science, Kyushu University, 3-1-l Maidashi, Higashi-ku, Fukuoka 812-8582, Japan.

Phone: +81-92-642-6325

Fax: +81-92-642-6329

E-mail: kiyo@dent.kyushu-u.ac.jp

Key words: Clear cell SCC, Tongue, p63, ARL4C, OSCC

Abstract

Clear cell squamous cell carcinoma (CCSCC), where cells show abundant clear cytoplasm, is a variant of squamous cell carcinoma (SCC) and a rare entity in the oral cavity. The characteristics of CCSCC, especially in immunohistochemical features, remain unclear. We characterized a case of CCSCC arising from the oral mucosal epithelium of tongue, where the clear cell lesion accounted for a predominant portion of the tumor. This CCSCC, which was partially surrounded by conventional SCC, exhibited cellular atypia immunohistopathologically and histopathologically with a high Ki-67 index, increased number of mitotic figures and enlarged nuclei. Intravascular invasion of the carcinoma cells was also observed. Furthermore, the CCSCC recurred and metastasized to the cervical lymph nodes and both lungs three months after resection. Immunohistochemical analyses demonstrated decreased expression of p40 (an isoform of SCC marker p63), ADP-ribosylation factor (ARF)-like 4c (ARL4C), yes-associated protein (YAP) and 5-methylcytosine (5mC) in the CCSCC lesion compared with the surrounding SCC lesion, where the expression of ARL4C was upregulated compared with non-tumor region and YAP showed nuclear translocation. In addition, siRNA loss-of-function experiments revealed that p63 expression was required for ARL4C expression and DNA methylation was induced by p63 and YAP/transcriptional co-activator with PDZ-binding motif (TAZ) signaling in oral SCC cell lines. These results suggest that CCSCC, in which several markers of SCC-associated intracellular signaling pathways are downregulated, together with evidence of altered epigenetic regulation, is characterized as an undifferentiated SCC variant.

1. Introduction

Oral squamous cell carcinoma (OSCC) is a carcinoma with squamous differentiation arising from the mucosal epithelium [1]. OSCC accounts for more than 90% of oral cancers [1]. Histopathologically, SCC is categorized into three grades based on the keratinization and degree of anaplasia: well-, moderately and poorly differentiated [1]. There are multiple subtypes of SCC including basaloid, spindle cell, adenosquamous, verrucous, papillary, acantholytic, lymphoepithelial and cuniculatum variants [1]. There are few major driver events identified in OSCC, resulting in lack of molecular targets of anti-tumor therapy for OSCC [2]. Therefore, other unknown molecular mechanisms may be involved in OSCC tumorigenesis. Abnormally activated intracellular signaling pathways may be involved in OSCC tumorigenesis, and such pathways may be potential targets for anti-tumor therapy for OSCC. In line with this hypothesis, accumulating evidence suggests that several activated intracellular signaling molecules, such as ADP-ribosylation factor (ARF)-like 4c (ARL4C) [3], yes-associated protein (YAP) [4,5] and Keratin 17 (KRT17) [6], may be not only specific markers of OSCC but also exerting an oncogenic role in OSCC tumorigenesis.

Clear cell SCC (CCSCC) is a rare entity [7], and to our knowledge, only six cases of CCSCC developed in the oral cavity has been reported to date (Table 1) [8-13]. CCSCC cells have clear cytoplasm in hematoxylin-eosin (HE) stained sections [11]. Various substances, such as glycogen, lipids, mucopolysaccharides, immature zymogen granules and water, seem to be accumulated in the cytoplasm of CCSCC cells [14]. The diagnosis of CCSCC is based on histopathlogical and immunohistological findings. In addition, special stains, such as Periodic Acid-Schiff (PAS) and mucicarmine, are important for making diagnostic decision. However, the characteristics of CCSCC, including its immunohistochemical features, such as ARL4C, YAP and KRT17 expression, are unclear, as the number of reports concerning CCSCC is limited (Table 1) [8-13].

In the present report, we characterized a case of CCSCC arising from the tongue using pathological specimens and OSCC cell lines.

2. Material and methods

2.1. Immunohistochemistry

The protocol for this study was approved by the ethical review board of the Local Ethical Committee of Kyushu University, Japan (#30-235). All specimens were fixed in 10% (v/v) neutral buffered formalin solution and embedded in paraffin blocks. Subsequently, the paraffin-embedded specimens were cut into 4-μm-thick sections, stained with HE, and examined by 3 experienced pathologists to confirm the diagnoses. Immunohistochemical staining was performed on 5-μm-thick paraffin sections. Antigen retrieval, elimination of the endogenous peroxide activity, and blocking were carried out as previously described [15,16]. The sections were then incubated with each primary antibody (used at 1:100 for Ki-67, used at 1:5 for AE1/AE3, used at 1:200 for p40, used at 1:200 for CK13, used at 1:200 for CK17, used at 1:100 for ARL4C, used at 1:300 for YAP, used at 1:100 for 5mC, used at 1:100 for CK5/6, used at 1:2 for S-100, used at 1:300 for SMA) at 4°C overnight. The details of the antibodies used are mentioned below. The sections were incubated with secondary antibody (Histofine Simple Stain MAX PO, Nichirei, Tokyo, Japan) for 1 h at room temperature. The immunoreactivity was visualized with a DAB substrate solution (Nichirei). Subsequently, the sections were counterstained with hematoxylin.

2.2. Cell lines and reagents

Human OSCC cell lines HSC-2, HSC-3 and SAS (Japanese Cancer Research Resources Bank) [16], and human cervical carcinoma cell line HeLaS3 [17] were used in this study. HSC-2 and HSC-3 were maintained in α-MEM (Invitrogen, Carlsbad, CA, USA), and SAS and HeLaS3 were maintained in D-MEM (Invitrogen). These culture media were supplemented with 10% fetal bovine serum (FBS) (Invitrogen) and contained 100 IU/ml penicillin and 100 mg/ml

streptomycin (Invitrogen). All of these cell lines were incubated at 37°C in a 5% CO_2 atmosphere.

Anti-Ki-67 (M7240), anti-AE1/AE3 (IR053), anti-CK13 (M7003), anti-CK17 (M7046), anti-CK5/6 (N7237) and anti-S-100 (IR504) antibodies, all of which were used for immunohistochemistry, were obtained from Dako (Carpentaria, CA, USA). Anti-p40 (ab172731) (for immunohistochemistry), anti-p63 (ab735) (for western blotting) and anti-double strand (ds) DNA (ab27156) (for dot blot) antibodies were obtained from Abcam (Cambridge, UK). Anti-ARL4C (HPA028927) (for immunohistochemistry and western blotting) antibody was obtained from Atlas antibodies (Voltavägen, SWE). Anti-YAP (sc-101199) (for immunohistochemistry) antibody was obtained from Santa Cruz Biotechnology (Dallas, TX, USA). Anti-5mC (39649) (for immunohistochemistry and dot blot) antibody was obtained from Active Motif (Carlsbad, CA, USA). Anti-YAP/TAZ (8418S) (for western blotting) antibody was obtained from Cell Signaling Technology (Beverly, MA, USA). Anti-β-actin (A5441) (for western blotting) antibody was obtained from Sigma-Aldrich (Steinheim, Germany).

2.3. Knockdown of protein expression by siRNA and quantitative RT-PCR

The effects of protein knockdown by siRNA were analyzed as previously described [17]. In brief, siRNAs (final conc. 20 nM) were transfected into OSCC cells using Lipofectamine RNAiMAX (Invitrogen). The following target sequences were used: randomized control, 5′-CAGTCGCGTTTGCGACTGG-3′, human p63 #1, 5′-GCTTAATCTTCAAAGCCTT-3′, human p63 #2, 5′-GCAGAACTGTAGCTGCCAT-3′, human YAP, 5′-GCATGACAGAAATAAGCTT-3′ and human TAZ, 5′-CCCAACAGACCCGTTTCCCUGATTT-3′. The transfected cells were then used for experiments conducted at 48 h post-transfection.

Quantitative RT-PCR was performed as described previously [3,18]. Forward and reverse primers were as follows: human ARL4C, 5′-CTAACATCTCGGCCTTCCAG-3′ and 5′-TCTGCTTGAGGGACTTCCTG-3′; human p63, 5′-GAAACGTACAGGCAACAGCA-3′ and 5′-GCTGCTGAGGGTTGATAAGC-3′; human p40, 5′-AAGGAGGCGAGGTTCTAAGC-3’ and 5′-AAGAGCCTCTGCTGCTTTTG-3′; human CTGF, 5′-CCGTACTCCCAAAATCTCCA-3’ and 5′-GTAATGGCAGGCACAGGTCT-3′; human CYR61, 5′-TCCGAGGTGGAGTTGACGAG-3’ and 5′-AGCACTGGGACCATGAAGTTG -3′; human DNMT1, 5′-GAACGGTGCTCATGCTTACA-3’ and 5′-TGTAATCCTGGGGCTAGGTG-3′; human DNMT3a, 5′-AGCCCAAGGTCAAGGAGATT-3’ and 5′-CAGCAGATGGTGCAGTAGGA-3′; human DNMT3b, 5′-TTGAATATGAAGCCCCCAAG-3’ and 5′-GGTTCC AACAGCAATGGACT-3′; human GAPDH, 5′-GCACCGTCAAGGCTGAGAAC-3′ and 5′- TGGTGAAGACGCCAGTGGA-3′.

2.4. Analysis of Cistrome Data Browser database

ChIP-seq peaks of p63 and active histone modifications, such as H3K4me3, H3K27ac and H3K9ac, in the 5’-untranslated region of the *ARL4C* gene were analyzed using the Cistrome Data Browser database (http://cistrome.org/db/#/). In the database, p63; Tongue SCC [19], Keratinocyte [20], MCF-10A (human mammary gland epithelial cell) of which raw data was deposited in NCBI GEO under accession number (GSE3378511), H3K4me3; TE-7 (human esophageal squamous cell carcinoma cell) [21], KYSE-150 (human esophageal squamous cell carcinoma cell) [22], MCF-7 (human mammary gland epithelial cell) [23], MCF-10A [24], H3K27ac; TE-7 [25], MCF-7 [26], MCF-10A [27], H3K9ac; TE-7 [21], MCF-7 [28], MCF-10A of which raw data was deposited in NCBI GEO under accession number (GSM2258717) were used in this study. The consensus sequence of p63 was obtained from JASPAR web site (https://jaspar.genereg.net).

2.5. Dot blot analysis

Dot blot analysis was performed as previously described [3,29] with modification. Genomic DNA was diluted to 50 ng/μl in 20 μl total volume. Five μl of 0.5 M NaOH was added to each sample and then the samples were incubated at 95°C for 5 min. The samples were put on ice and neutralized with 2.5 μl of 6.6 M ammonium acetate. 2.75 μl of each mixture was spotted onto a nitrocellulose membrane and allowed to air dry for 10 min. The membrane was baked for 2 h at 80°C and blocked with 5% milk for 2 h at room temperature. Anti-5mC antibody (1:1000) or anti-ds DNA antibody (1:3000) was incubated at 4°C overnight, and subsequent incubation with goat anti-mouse IgG-HRP for 1 h. ECL Western Blotting Detection Reagents (GE Healthcare, Little Chalfont, UK) were used for detection. Dot blot intensities were analyzed using Image J (Version 1.63, NIH, Bethesda, MD).

2.6. Statistical analysis

Significant differences were determined using one-way ANOVA with *post hoc* Tukey test. *P* value of < 0.05 or 0.01 was considered statistically significant.

3. Results

3.1. Clinical features and histological findings

A 70-year-old male visited at the Department of Oral and Maxillofacial Surgery at Kyushu University Hospital (Fukuoka, Japan) with a mass showing exophytic growth on the right ventral surface of the tongue without apparent subjective symptoms (Fig. lA). The patient had been followed up for thrombocytopenic purpura. An oral examination revealed that the 11×10-mm tumor mass was soft-elastic and well-circumscribed without induration, and the overlying mucosal surface showed extensive erosion and partial hemorrhage. Contrast-enhanced computed tomography (CT) and positron emission tomography (PET)-CT showed an enhanced lesion on the right side of the tongue (data not shown). No distant metastasis was evident in the clinical findings with PET-CT or abdominal ultrasonography (data not shown). Based on the examinations, the lesion was clinically diagnosed as a malignant tumor arisen from tongue.

The patient had a history of OSCC in the left tongue and left buccal mucosa, and both lesions had been diagnosed as well-differentiated SCC and treated with resection, left neck dissection and radiation therapy 20 years ago and resection 5 years ago, respectively. He had undergone regular follow-up without local recurrence or metastasis. Therefore, the right tongue tumor seemed to be a primary malignant tumor, clinically. Cytology from the lesion revealed that scattered or clusters of carcinoma cells with high nucleo-cytoplasmic (N/C) ratio, hyperchromatic large nuclei and prominent nucleoli (data not shown). Cytologists and pathologists discussed the cytological findings and judged them to be indicative of malignancy. Resection with a 1-cm surgical safety margin was therefore performed. HE-stained sections showed exophytic and invasive growth of atypical clear cells with sheet- and island-like appearances into the muscular layer (Fig. 1B; upper panel). The clear cells showed abundant clear cytoplasm along with enlarged and centrally placed rounded nuclei (Fig. 1B-3, C and E). The number of mitotic figures in the atypical clear cells was 4.3 per 4 high-power fields in the

lesion (data not shown). In addition, the atypical clear cells were negative for PAS, Alcian-blue and mucicarmine stainings (data not shown), suggesting that accumulation of water and/or hydropic change had occurred in the cytoplasm of the atypical clear cells. Based on these findings and the immunohistochemical observations mentioned below, the clear cell lesion was diagnosed as a CCSCC. The CCSCC lesion (Fig. 1B-3) was partially surrounded with a conventional SCC lesion (Fig. 1B-2, 5), which was also connected to a non-tumor squamous cell region (Fig. 1B-1), suggesting that the clear cell lesion might have developed from the SCC lesion. Intravascular invasion of the carcinoma cells was also observed (Fig. 1B-4). The clear cell lesion accounted for a predominant portion (90%) of this tumor (Fig. 1D).

The CCSCC recurred three months after resection. HE-stained sections of the recurrence lesion showed invasive growth of the atypical clear cells with sheet- and strand-like appearances. The clear cells had abundant clear cytoplasm (Fig. 1E), enlarged nuclei and a high Ki-67 index (data not shown). In addition, the atypical clear cells were negative for PAS, Alcian-blue and mucicarmine stainings. Squamous differentiation was observed in a limited region (data not shown). The immunohistochemical features were similar to those of the primary CCSCC (data not shown). Based on these findings, the clear cell lesion was diagnosed as recurrent CCSCC. In addition, metastasis to the right cervical lymph nodes was detected by ultrasonography. PET-CT also indicated metastasis to both lungs as well as the cervical lymph node (data not shown).

3.2. Characterization of the CCSCC by an immunohistochemical analysis

To clarify the characterization of CCSCC, immunohistochemical analyses were carried out. The Ki-67 labeling index was 38.8% and 26.3% in the CCSCC and SCC lesion, respectively, which showed a significant difference ($P = 0.02$) (Fig. 2 and Fig. S1). Immunohistochemical analyses showed that the CCSCC cells were positive for AE1/AE3 (Fig. 2), weakly positive for CK5/6

(data not shown) and CK17, and negative for CK13 (Fig. 2). In contrast, the surrounding SCC cells were positive for AE1/AE3 (Fig. 2), CK5/6 (data not shown) and CK17, and negative for CK13 (Fig. 2). These results suggested that the CCSCC cells might be malignant cells bearing the characteristics of SCC. In addition, similar to previous reports (Table 1), S-100 and smooth muscle actin (SMA) were negative in the CCSCC and SCC lesions immunohistochemically (data not shown). Interestingly, the intensity of p40, which is an isoform of p63 [30], in CCSCC lesion was decreased compared with the SCC lesion (Fig. 2). P63 and p40 are useful markers for SCC variants [31]. These immunohistochemical findings suggested that CCSCC exhibits similar characters to SCCs but is not completely coincident with the SCC.

To further profile the CCSCC, additional immunohistochemical analyses were performed. ARL4C, the expression of which is upregulated in several tumors by multiple mechanisms in a cell-context-dependent manner, is associated with tumorigenesis [3,17,32-38]. The expression of ARL4C in the CCSCC lesion was decreased compared with the SCC lesion (Fig. 3). ARL4C was hardly detected in the non-tumor region consistent with previous reports [3,38] (Fig. 3). The Hippo pathway regulates cell proliferation through the nuclear translocation of major downstream effectors, YAP and TAZ, resulting in the induction of target gene transcription [39,40]. Consistent with a previous report [5], YAP was localized in the nucleus of the SCC cells, whereas it was hardly detected at all in the CCSCC cells (Fig. 3 and Fig. S2). The intensity of 5mC, which is a marker for global DNA methylation and whose loss through conversion to 5-hydroxymethylcytosine (5hmC) is associated with tumorigenesis [41], was decreased in the CCSCC lesion (Fig. 3). Furthermore, lower expression of ARL4C, YAP and 5mC was observed in clear cell lesion compared to that in SCC lesion in the additional cases, where clear cells with enlarged and centrally placed rounded nuclei were focally observed in the section (Case 1; 1.5 % and Case 2; 1.4 %, respectively) (Fig. S3). These results suggest that at least two kinds of intracellular signaling pathways, such as ARL4C signaling and YAP

signaling, are downregulated, and epigenetic alteration may occur in the CCSCC lesion compared with the SCC lesion.

3.3. Effects of p63 on ARL4C expression in OSCC cells

P63, which is a marker of SCC together with p40, reportedly suppresses squamous differentiation [31]. As the expression of p40 in the CCSCC lesion was decreased compared with that in the SCC lesion (Fig. 2), we investigated the function of p63 using OSCC cells. We measured the *ARL4C* and *p63* mRNA levels in three human OSCC cell lines and a control human cervical carcinoma cell line, HeLaS3. The OSCC cell lines showed higher levels of *ARL4C* and *p63* than the HeLaS3 cells (Fig. 4A). When p63 was knocked down by two different siRNAs (Fig. 4B), levels of p63, p40 and ARL4C were decreased (Fig. 4B and C), but the expression of YAP/TAZ was not changed (Fig. S4). These data suggested that p63 could specifically regulate the ARL4C expression in OSCC cells. In addition, the Cistrome Data Browser database indeed showed ChIP-seq peaks of p63 and active histone modifications, such as H3K4me3, H3K27ac and H3K9ac, in the 5'-untranslated region of the *ARL4C* gene (Fig. 4D). These results suggest that p63 may be involved in the regulation of ARL4C expression in OSCC cells.

To further analyze the function of p63 in the OSCC cells, we examined the morphological changes in the p63 knock-down OSCC cells. Although p63 knock-down did not affect the cell size or shape, the size of nuclei was more enlarged in p63 knock-down OSCC cells than in control cells (Fig. 4E), which was similar to that observed in the CCSCC (see Fig. 1B-2, 3 and 1C).

3.4. The effects of p63 and YAP/TAZ on DNA methylation status in OSCC cells

Recent reports reveled that p63 or YAP/TAZ regulates DNA methylation status through several mechanisms, such as protein association through p63 with DNA methyltransferases (DNMTs) or regulation of DNMTs expression [42,43]. YAP/TAZ siRNA reduced the mRNA levels of ankyrin repeat domain 1 (*ANKRD1*) and cellular communication network factor 1 (*CCN1*; also known as *CYR61*), which are transcriptional targets of YAP/TAZ [5], while YAP/TAZ siRNA did not affect the expression of p63 in OSCC cells (Fig. 5A). Together with the data of p63 siRNA treatment (see Fig S4), p63 and YAP/TAZ appear to be independent intracellular signaling pathways at least in OSCC cells. Finally, the effects of p63 and/or YAP/TAZ on DNA methylation status were examined in OSCC cells. Although sip63 or siYAP/TAZ did not affect 5mC levels, the simultaneous suppression of p63 and YAP/TAZ signaling dramatically reduced 5mC levels (Fig. 5B). In addition, knockdown of p63 and YAP/TAZ specifically decreased *DNMT1* expression among *DNMT*s (Fig. 5C). These data indicated that p63 signaling and YAP/TAZ signaling might be cooperatively involved in regulation of DNA methylation in OSCC cells.

4. Discussion

CCSCC is an extremely rare entity that was first described in the skin [7]. In the present study, we characterized CCSCC arising from the tongue using immunohistochemical analyses. To date, only six cases of CCSCC have been reported in the oral cavity (Table 1) [8-13], to our knowledge. Among them, five reports demonstrated that the CCSCC cells showed cellular atypia and nuclear pleomorphism with irregular mitotic figures and hyperchromatic nucleus. Consistently, our present study showed that the CCSCC exhibited cellular atypia with an elevated Ki-67 index, increased number of mitotic figures and enlarged nucleus, and intravascular invasion of the carcinoma cells. Furthermore, the recurrence of CCSCC with distant metastasis was observed three months later after resection. These findings suggest that the current CCSCC case may have high-grade malignant potential, thereby resulting in a poor prognosis. Consistently, a previous report showed that CCSCC with perineural invasion metastasized to the lung three months later after surgery [11]. In addition, two other cases had cervical lymph node metastasis [9,12], and another case recurred [13]. The presence of metastasis and/or recurrence was unclear in the two remaining cases (Table 1). Therefore, CCSCC should be considered as a noteworthy SCC variant clinically as well as histopathologically.

In the oral cavity, tumors with clear cells can be classified into three categories: malignant tumors of the salivary gland, odontogenic tumors and metastatic tumors. First, malignant tumors of salivary gland, including mucoepidermoid carcinoma, acinic cell carcinoma, clear cell carcinoma, myoepithelial carcinoma and epithelial-myoepithelial carcinoma (EMC), were considered in the differential diagnosis of the clear cell lesion [44] in the present case. Mucoepidermoid carcinoma, which is composed of mucous, intermediate and epidermoid cells, is the most common salivary gland malignancy [44]. Acinic cell carcinoma demonstrates serous acinar cell differentiation characterized by cytoplasmic zymogen secretory

granules [44,45]. In the present case of CCSCC, the findings of negative staining with mucicarmine and PAS ruled out mucoepidermoid carcinoma, acinic cell carcinoma and clear cell carcinoma. Myoepithelial carcinoma is a malignancy composed entirely of neoplastic myoepithelial cells [44]. EMC is a rare neoplasm of salivary gland and low-grade tumor [44,46]. EMC has a biphasic pattern composed of a nest of inner luminal ductal cells and outer abluminal myoepithelial cells [47]. Histopathological findings and negative stainings for S-100 and SMA differentiated CCSCC from myoepithelial carcinoma and EMC. Second, odontogenic tumors with clear cells include clear cell odontogenic carcinoma (CCOC), odontogenic ghost cell tumor (OGCT) and calcifying epithelial odontogenic tumor (CEOT) [12,14]. As the present CCSCC arose from the tongue, and odontogenic tumors usually occur in the maxillary and mandibular bones, odontogenic tumors were ruled out. Furthermore, CCOC is distinguished by negative PAS staining. OGCT, which involves aberrant keratinization with ghost cells, was able to be excluded based on the histopathological finding. CEOT is a benign epithelial odontogenic tumor that secretes an amyloid protein and Liesegang ring calcifications [48], neither of which was observed in our case. Finally, metastatic tumors, especially those from the breast and kidney, were also considered. However, general examinations, including PET-CT, chest X-ray and abdominal ultrasonography, did not indicate primary tumors in the other organs, including the kidney, in our case.

ARL4C is reportedly highly expressed in the lesion of various tumors [3,32,33, 35,38,49]. Consistently, the expression of ARL4C was elevated in the SCC lesion partially surrounding the CCSCC lesion. The expression of ARL4C is regulated by Wnt/β-catenin signaling, the Ras/MAP kinase pathway [17,32,35,38] and DNA methylation [3]. We first demonstrated p63 could be involved in ARL4C expression in OSCC. Since a previous report showed that p63 overexpression is correlated with a poor survival rate in OSCC [50] and an elevated ARL4C expression promotes OSCC tumorigenesis [3], the function of p63-mediated

ARL4C in OSCC tumorigenesis needs to be clarified. In addition, the present study indicated that p63 signaling could regulate nuclear size. Abnormal variation in nuclear size, which is observed even in oral epithelial dysplasia [1], is an important index for making a diagnosis of malignant tumors. Therefore, further study is needed to elucidate the precise mechanism by which p63 regulates the nuclear size.

A report demonstrated that the lower level of 5mC could be a poor prognosis factor in glioblastoma multiforme [51], consistent with our case with poor prognosis. Reportedly, p63 and/or YAP/TAZ could regulate DNA methylation at the protein or transcriptional level [42,43], and our present data demonstrated that p63 and YAP/TAZ cooperatively regulated DNA methylation in OSCC cells (see Fig. 5B). Functional interaction of p63 with YAP has also been demonstrated [52]. While the mechanisms regulating DNA methylation may depend on a cell-context-dependent manner, it is intriguing to speculate that DNA methylation status, which is regulated by p63 and YAP/TAZ in OSCC cells, might be a novel poor prognosis marker in OSCC.

ARL4C, YAP and 5mC were hardly detected in the CCSCC lesion. These immunohistochemical findings suggest that at least two kinds of independent intracellular signaling pathways, such as ARL4C signaling and YAP signaling, were downregulated, which is likely to be associated with undifferentiated status and altered epigenetic regulation in the CCSCC lesion. The CCSCC lesion might have originated from the SCC lesion considering the histopathological location (see Fig 1B-5), the immunohistochemical characteristics (see Fig. 2) and the *in vitro* experiments, in which the decreased expression of p63 and YAP/TAZ in OSCC cells (see Fig 4B, 4C, 4D, 5B and 5C) mirrored the immunohistochemical findings in CCSCC patients (see Figs. 2 and 3). Given our results, we speculated that the CCSCC could be an undifferentiated SCC, with altered intracellular signaling and epigenetic regulation. It is important to characterize this rare variant of SCC and to discriminate the lesion from the tumors

with clear cells, such as other salivary gland tumors, odontogenic tumors and metastatic tumors [53]. No specific markers for CCSCC have yet been established, so novel specific markers for CCSCC are needed to make a correct diagnosis, as CCSCC can have high-grade malignant potential.

In summary, we characterized a case of CCSCC with high malignant potential arising from the mucosal epithelium of the tongue by immunohistochemical analyses and proposed that the CCSCC might be undifferentiated SCC, with altered intracellular signaling and epigenetic regulation.

Figure legends

Figure l. Clinical features and histological findings of CCSCC.

(A) A macroscopic photograph of the tongue at the initial visit. The well-circumscribed elastic soft, 11x10-mm mass was overlaid on the right ventral surface of the tongue. Arrowheads indicate the mass. (B) HE staining of the non-tumor region, SCC lesion and CCSCC lesion (top right panel). The numbered boxes in the low-power image show enlarged images (second panels from the top). The dotted boxes are further enlarged images (third panels from the top). The black arrowheads indicate intravascular invasion of the carcinoma cells in B-4. The black line indicates the border between clear cell lesion and squamous cell carcinoma lesion in B-5. (C) The nucleus areas in non-tumor region, SCC and clear cell lesion were measured. (D) The SCC and CCSCC area proportions in the tumor were measured. (E) HE staining showing CCSCC cells in the primary lesion and the recurrent lesion. Scale bars, 500 μm (B), 100 μm (B-1, 2, 3) (upper panels) 20 μm (B-1, 2, 3 (lower panels), 4, 5 and E).

Figure 2. Characterization of CCSCC by immunohistochemical analysis.

The CCSCC lesion was stained with anti-Ki-67, anti-AE1/AE3, anti-CK-17, anti-CK13 and anti-p40 antibodies, and hematoxylin. Scale bars, 50 μm.

Figure 3. Characterization of CCSCC with undifferentiated status by an immunohistochemical analysis.

The CCSCC lesion was stained with anti-ARL4C, anti-YAP, and anti-5mC antibodies as well as hematoxylin. Insets are further enlarged images. Scale bars, 50 μm.

Figure 4. The effects of p63 on ARL4C expression in oral squamous cell carcinoma cells.

(A) *ARL4C* and *p63* mRNA levels were measured in OSCC cell lines (HSC-2, HSC-3 and

SAS cells) and HeLaS3 cells by quantitative RT-PCR. Relative levels of *ARL4C* and *p63* mRNA expression were normalized to *GAPDH* and are presented as fold-changes compared with the expression in control HeLaS3 cells. (B and C) HSC-2, HSC-3 and SAS cells were transfected with control or two different p63 siRNAs and analyzed 48 h post-transfection. (B) *p63*, *p40* and *ALR4C* mRNA levels were measured by quantitative RT-PCR. Relative *p63*, *p40* and *ALR4C* mRNA levels normalized by *GAPDH* are presented as fold-changes compared with levels in control siRNA transfected cells. **1, **2 and **3 indicate significant difference in the comparison of p63, p40 and ARL4C, respectively. (C) Protein samples were analyzed by western blotting using anti-ARL4C, anti-p63, and anti-β-actin antibodies. (D) Genomic views of p63, H3K4me3, H3K27ac and H3K9ac ChIP enrichments at the human *ARL4C* gene obtained from the Cistrome Data Browser database. The *ARL4C* gene contains one predicted p63-binding site. (E) HSC-2, HSC-3 and SAS cells were transfected with control or p63 siRNA for 48 h. The cells were stained with Hoechst 33342 and phalloidin, and then the areas of the nucleus were calculated. Scale bars, 50 μm. Results are shown as means ± s.d. of three independent experiments. *P<0.05, **P<0.01.

Figure 5. The effects of p63 and YAP/TAZ on DNA methylation status in oral squamous cell carcinoma cells.

(A and B) HSC-3 and SAS cells were transfected with control, p63 or YAP/TAZ siRNAs and analyzed 48 h post-transfection. (A) Protein samples were analyzed by western blotting using anti-YAP/TAZ, anti-p63, and anti-β-actin antibodies (left panels). *CTGF* and *Cyr61* mRNA levels were measured by quantitative RT-PCR. Relative levels of *CTGF* and *Cyr61* mRNA expression normalized to *GAPDH* are presented as fold-changes compared with levels in control siRNA transfected cells. (B) Analysis of 5mC levels in genomic DNA isolated from p63 and/or YAP/TAZ knock-down HSC-3 and SAS was performed by dot blot assay using an anti-

5mC antibody. Anti-ds DNA antibody was probed as a control. Dot intensities were quantified using NIH image software and the ratio of 5mC/ds DNA is presented as fold-change compared with control siRNA transfected cells. (C) HSC-3 and SAS cells were transfected with control, p63 and YAP/TAZ siRNAs and analyzed 48 h post-transfection. *DNMT1*, *DNMT3a* and *DNMT3b* mRNA levels were measured by quantitative RT-PCR. Relative *DNMT1*, *DNMT3a* and *DNMT3b* mRNA levels were normalized to *GAPDH* and are presented as fold-changes compared with levels in control siRNA transfected cells. Results are shown as means ± s.d. of three independent experiments. **P*<0.05, ** *P*<0.01.

Funding: This work was supported by JSPS KAKENHI Grants to K.H. (2021-2023) (JP21K09843), S.F. (2020-2022) (JP20K09906) and T.K. (2020-2022) (JP20K10096), and Takeda Science Foundation to K.H. and S.F., SGH Foundation to S.F. and Qdai-jump Research Program to K.H.

Conflict of Interest Disclosures: None of the authors have any relevant financial relationship(s) with a commercial interest.

Ethics approval and consent to participate

This study was approved by the Research Ethics Committee of Kyushu University (approval nos. 30-235). Written informed consent was obtained from the patient.

Patient consent for publication

The patient provided written informed consent for the publication of the case and any associated images.

Author contributions

Kana Hasegawa: Investigation, Writing - Original Draft, Funding acquisition.: **Shinsuke Fujii:** Conceptualization, Methodology, Writing - Review & Editing, Funding acquisition.: **Kari J Kurppa:** Supervision.: **Takashi Maehara, Kazunari Oobu, Seiji Nakamura:** Resources.: **Tamotsu Kiyoshima:** Project administration, Writing - Review & Editing, Funding acquisition. All authors were involved in writing the paper and had final approval of the submitted and published versions.

Acknowledgments

The authors thank Dr. M. Sakamoto for searching clinical information in this research, Drs. H. Wada, R. Nagano, M. Kokura and Mr H. Otoba, Ms. M. Egami and Mr. N. Hayama for valuable technical support in this research.

References

[1] A.K. El-Nagger, J.K.C. Chan, J.R. Grandis, T. Takata, P.J. Slootweg. Malignant surface epithelial tumours, WHO classification of Head and Neck Tumours, (4th ed.,), IARC press, Lyon (2017), pp. 106-113

[2] The Cancer Genome Atlas Network. Comprehensive genomic characterization of head and neck squamous cell carcinomas. Nature. 517 (2015) 576-82. https://doi.org/ 10.1038/nature14129.

[3] Fujii S, Shinjo K, Matsumoto S, Harada T, Nojima S, Sato S, Usami Y, Toyosawa S, Morii E, Kondo Y, Kikuchi A, Epigenetic upregulation of ARL4C, due to DNA hypomethylation in the 3'-untranslated region, promotes tumorigenesis of lung squamous cell carcinoma, Oncotarget 7 (2016) 81571-87. https://doi.org/10.18632/oncotarget.13147.

[4] Omori H, Nishio M, Masuda M, Miyachi Y, Ueda F, Nakano T, Sato K, Mimori K, Taguchi K, Hikasa H, Nishina H, Tashiro H, Kiyono T, Mak TW, Nakao K, Nakagawa T, Maehama T, Suzuki A, 2020. YAP1 is a potent driver of the onset and progression of oral squamous cell carcinoma, Sci Adv. 6:eaay3324. https://doi.org/10.1126/sciadv.aay3324.

[5] Hasegawa K, Fujii S, Matsumoto S, Tajiri Y, Kikuchi A, Kiyoshima T, YAP signaling induces PIEZO1 to promote oral squamous cell carcinoma cell proliferation, J Pathol 253 (2021) 80-93. https://doi.org/10.1002/path.5553.

[6] Mikami Y, Fujii S, Nagata K, Wada H, Hasegawa K, Abe M, Yoshimoto RU, Kawano S, Nakamura S, Kiyoshima T, GLI-mediated Keratin 17 expression promotes tumor cell growth through the anti-apoptotic function in oral squamous cell carcinomas, J Cancer Res Clin Oncol 143 (2017) 1381-93. https://doi.org/10.1007/s00432-017-2398-2.

[7] Kuo T, Clear cell carcinoma of the skin. A variant of the squamous cell carcinoma that simulates sebaceous carcinoma, Am J Surg Pathol 4 (1980) 573-83. https://doi.org/10.1097/00000478-198012000-00008.

[8] Frazier JJ, Sacks H, Freedman PD, Primary glycogen-rich clear cell squamous cell carcinoma of the mandibular gingiva, Oral Surg Oral Med Oral Pathol Oral Radiol 114 (2012) e47-51. https://doi.org/10.1016/j.oooo.2012.01.033.

[9] Nainani P, Singh HP, Paliwal A, Nagpal N, A rare case report of clear cell variant of oral squamous cell carcinoma, J Clin Diagn Res 8 (2014) Qd07-9. https://doi.org/10.7860/JCDR/2014/11536.5339.

[10] Kaliamoorthy S, Sethuraman V, Ramalingam SM, Arunkumar S, A rare case of clear cell variant of oral squamous cell carcinoma, J Nat Sci Biol Med 6 (2015) 245-7. https://doi.org/10.4103/0976-9668.149209.

[11] Khoury ZH, Bugshan A, Lubek JE, Papadimitriou JC, Basile JR, Younis RH, Glycogen-Rich Clear Cell Squamous Cell Carcinoma Originating in the Oral Cavity, Head Neck Pathol 11(2017) 552-60. https://doi.org/10.1007/s12105-017-0812-3.

[12] Devi A, Kamboj M, Singh V, Singh S, Clear-cell variant of squamous cell carcinoma in

maxilla as primary lesion: A rare case, J Oral Maxillofac Pathol 21 (2017) 425-8. https://doi.org/10.4103/jomfp.JOMFP_180_16

[13] Ramani P, Gheena S, Karunagaran M, Hannah R, Clear-cell variant of oral squamous cell carcinoma: A rare entity, J Oral Maxillofac Pathol 25 (2021) S22-s6. https://doi.org/10.4103/jomfp.JOMFP_295_20

[14] Premalatha BR, Neethi H, Clear Cell Tumors of the Head and Neck, An Overview. World Journal of Dentistry 3 (2012) 344-9.

[15] Mikami Y, Fujii S, Kohashi KI, Yamada Y, Moriyama M, Kawano S, Nakamura S, Oda Y, Kiyoshima T,Low-grade myofibroblastic sarcoma arising in the tip of the tongue with intravascular invasion, A case report, Oncol Lett 16 (2018) 3889-94. https://doi.org/10.3892/ol.2018.9115.

[16] Fujii S, Tajiri Y, Hasegawa K, Matsumoto S, Yoshimoto RU, Wada H, Kishida S, Kido MA, Yoshikawa H, Ozeki S, Kiyoshima T, The TRPV4-AKT axis promotes oral squamous cell carcinoma cell proliferation via CaMKII activation, Lab Invest 100 (2020) 311-23. https://doi.org/10.1038/s41374-019-0357-z.

[17] Matsumoto S, Fujii S, Sato A, Ibuka S, Kagawa Y, Ishii M, Kikuchi A, A combination of Wnt and growth factor signaling induces Arl4c expression to form epithelial tubular structures, EMBO J 33 (2014) 702-18. https://doi.org/10.1002/embj.201386942.

[18] Fujii S, Nagata K, Matsumoto S, Kohashi KI, Kikuchi A, Oda Y, Kiyoshima T, Wada N, Wnt/β-catenin signaling, which is activated in odontomas, reduces Sema3A expression to regulate odontogenic epithelial cell proliferation and tooth germ development, Sci Rep 9 (2019) 4257. https://doi.org/10.1038/s41598-019-39686-1.

[19] Sastre-Perona A, Hoang-Phou S, Leitner MC, Okuniewska M, Meehan S, Schober M, De Novo PITX1 Expression Controls Bi-Stable Transcriptional Circuits to Govern Self-Renewal and Differentiation in Squamous Cell Carcinoma, Cell Stem Cell 24 (2019), 390-404.e8. https://doi.org/10.1016/j.stem.2019.01.003

[20] Zarnegar BJ, Webster DE, Lopez-Pajares V, Vander Stoep Hunt B, Qu K, Yan KJ, Berk DR, Sen GL, Khavari PA, Genomic profiling of a human organotypic model of AEC syndrome reveals ZNF750 as an essential downstream target of mutant TP63, Am J Hum Genet 91 (2012), 435-43. https://doi.org/10.1016/j.ajhg.2012.07.007

[21] Rochman M, Kartashov AV, Caldwell JM, Collins MH, Stucke EM, Kc K, Sherrill JD, Herren J, Barski A, Rothenberg ME, Neurotrophic tyrosine kinase receptor 1 is a direct transcriptional and epigenetic target of IL-13 involved in allergic inflammation, Mucosal Immunol 8 (2015), 785-98. https://doi.org/10.1038/mi.2014.109

[22] Pedersen MT, Agger K, Laugesen A, Johansen JV, Cloos PA, Christensen J, Helin K, The demethylase JMJD2C localizes to H3K4me3-positive transcription start sites and is dispensable for embryonic development, Mol Cell Biol 34 (2014), 1031-45. https://doi.org/10.1128/MCB.00864-13

[23] Jozwik KM, Chernukhin I, Serandour AA, Nagarajan S, Carroll JS, FOXA1 Directs H3K4 Monomethylation at Enhancers via Recruitment of the Methyltransferase MLL3, Cell Rep 17 (2016), 2715-23. https://doi.org/10.1016/j.celrep.2016.11.028

[24] Dobson JR, Hong D, Barutcu AR, Wu H, Imbalzano AN, Lian JB, Stein JL, van Wijnen AJ, Nickerson JA, Stein GS, Identifying Nuclear Matrix-Attached DNA Across the Genome, J Cell Physiol 232 (2017), 1295-305. https://doi.org/ 10.1002/jcp.25596

[25] Jiang YY, Lin DC, Mayakonda A, Hazawa M, Ding LW, Chien WW, Xu L, Chen Y, Xiao JF, Senapedis W, Baloglu E, Kanojia D, Shang L, Xu X, Yang H, Tyner JW, Wang MR, Koeffler HP, Targeting super-enhancer-associated oncogenes in oesophageal squamous cell carcinoma, Gut 66 (2017), 1358-68. https://doi.org/ 10.1136/gutjnl-2016-311818

[26] Li W, Hu Y, Oh S, Ma Q, Merkurjev D, Song X, Zhou X, Liu Z, Tanasa B, He X, Chen AY, Ohgi K, Zhang J, Liu W, Rosenfeld MG, Condensin I and II Complexes License Full Estrogen Receptor α-Dependent Enhancer Activation, Mol Cell 59 (2015), 188-202. https://doi.org/ 10.1016/j.molcel.2015.06.002

[27] Rhie SK, Guo Y, Tak YG, Yao L, Shen H, Coetzee GA, Laird PW, Farnham PJ, Identification of activated enhancers and linked transcription factors in breast, prostate, and kidney tumors by tracing enhancer networks using epigenetic traits, Epigenetics Chromatin 9 (2016), 50. https://doi.org/ 10.1186/s13072-016-0102-4

[28] Joseph R, Orlov YL, Huss M, Sun W, Kong SL, Ukil L, Pan YF, Li G, Lim M, Thomsen JS, Ruan Y, Clarke ND, Prabhakar S, Cheung E, Liu ET, Integrative model of genomic factors for determining binding site selection by estrogen receptor-α, Mol Syst Biol 6 (2010), 456. https://doi.org/10.1038/msb.2010.109

[29] Gonzalez F, Zhu Z, Shi ZD, Lelli K, Verma N, Li QV, Huangfu D, An iCRISPR platform for rapid, multiplexable, and inducible genome editing in human pluripotent stem cells, Cell Stem Cell 15 (2014), 215-26. https://doi.org/ 10.1016/j.stem.2014.05.018

[30] Nobre AR, Albergaria A, Schmitt F, p40: a p63 isoform useful for lung cancer diagnosis - a review of the physiological and pathological role of p63, Acta Cytol 57 (2013) 1-8. https://doi.org/10.1159/000345245.

[31] Yang A, Schweitzer R, Sun D, Kaghad M, Walker N, Bronson RT, Tabin C, Sharpe A, Caput D, Crum C, McKeon F, p63 is essential for regenerative proliferation in limb, craniofacial and epithelial development, Nature 398 (1999) 714-8. https://doi.org/10.1038/19539.

[32] Fujii S, Matsumoto S, Nojima S, Morii E, Kikuchi A, Arl4c expression in colorectal and lung cancers promotes tumorigenesis and may represent a novel therapeutic target, Oncogene 34 (2015) 4834-44. https://doi.org/10.1038/onc.2014.402.

[33] Matsumoto S, Fujii S, Kikuchi A, Arl4c is a key regulator of tubulogenesis and tumourigenesis as a target gene of Wnt-beta-catenin and growth factor-Ras signalling, J Biochem 161 (2017) 27-35. https://doi.org/10.1093/jb/mvw069.

[34] Hu Q, Masuda T, Sato K, Tobo T, Nambara S, Kidogami S, Hayashi N, Kuroda Y, Ito S, Eguchi H, Saeki H, Oki E, Maehara Y, Mimori K, Identification of ARL4C as a Peritoneal Dissemination-Associated Gene and Its Clinical Significance in Gastric Cancer, Ann Surg Oncol 25 (2018) 745-53. https://doi.org/10.1245/s10434-017-6292-6.

[35] Harada T, Matsumoto S, Hirota S, Kimura H, Fujii S, Kasahara Y, Gon H, Yoshida T, Itoh T, Haraguchi N, Mizushima T, Noda T, Eguchi H, Nojima S, Morii E, Fukumoto T, Obika S, Kikuchi A, Chemically Modified Antisense Oligonucleotide Against ARL4C Inhibits Primary and Metastatic Liver Tumor Growth, Mol Cancer Ther 18 (2019) 602-12. https://doi.org/10.1158/1535-7163.MCT-18-0824.

[36] Chen Q, Weng HY, Tang XP, Lin Y, Yuan Y, Li Q, Tang Z, Wu HB, Yang S, Li Y, Zhao XL, Fu WJ, Niu Q, Feng H, Zhang X, Wang Y, Bian XW, Yao XH, ARL4C stabilized by AKT/mTOR pathway promotes the invasion of PTEN-deficient primary human glioblastoma, J Pathol 247 (2019) 266-78. https://doi.org/10.1002/path.5189.

[37] Kimura K, Matsumoto S, Harada T, Morii E, Nagatomo I, Shintani Y, Kikuchi A, ARL4C is associated with initiation and progression of lung adenocarcinoma and represents a therapeutic target, Cancer Sci 111 (2020) 951-61. https://doi.org/10.1111/cas.14303.

[38] Fujii S, Ishibashi T, Kokura M, Fujimoto T, Matsumoto S, Shidara S, Kurppa KJ, Pape J, Caton J, Morgan PR, Heikinheimo K, Kikuchi A, Jimi E, Kiyoshima T, RAF1-MEK/ERK pathway-dependent ARL4C expression promotes ameloblastoma cell proliferation and osteoclast formation, J Pathol 256 (2022) 119-33. https://doi.org/10.1002/path.5814.

[39] Saucedo LJ, Edgar BA, Filling out the Hippo pathway, Nat Rev Mol Cell Biol 8 (2007) 613-21. https://doi.org/10.1038/nrm2221.

[40] Meng Z, Qiu Y, Lin KC, Kumar A, Placone JK, Fang C, Wang KC, Lu S, Pan M, Hong AW, Moroishi T, Luo M, Plouffe SW, Diao Y, Ye Z, Park HW, Wang X, Yu FX, Chien S, Wang CY, Ren B, Engler AJ, Guan KL, RAP2 mediates mechanoresponses of the Hippo pathway, Nature 560 (2018) 655-60. https://doi.org/10.1038/s41586-018-0444-0.

[41] Song CX, He C, Balance of DNA methylation and demethylation in cancer development, Genome Biol 13 (2012) 173. https://doi.org/10.1186/gb-2012-13-10-2012.

[42] Rinaldi L, Datta D, Serrat J, Morey L, Solanas G, Avgustinova A, Blanco E, Pons JI, Matallanas D, Von Kriegsheim A, Di Croce L, Benitah SA, Dnmt3a and Dnmt3b Associate with Enhancers to Regulate Human Epidermal Stem Cell Homeostasis, Cell Stem Cell 19 (2016), 491-501. https://doi.org/10.1016/j.stem.2016.06.020

[43] Passaro F, De Martino I, Zambelli F, Di Benedetto G, Barbato M, D'Erchia AM, Manzari C, Pesole G, Mutarelli M, Cacchiarelli D, Antonini D, Parisi S, Russo T, YAP contributes to DNA methylation remodeling upon mouse embryonic stem cell differentiation, J Biol Chem 296 (2021), 100138. https://doi.org/10.1074/jbc.RA120.015896

[44] A.K. El-Nagger, J.K.C. Chan, J.R. Grandis, T. Takata, P.J. Slootweg. Tumours of salivary glands, WHO classification of Head and Neck Tumours, (4th ed.,), IARC press, Lyon

(2017), pp. 160-178

[45] Al-Zaher N, Obeid A, Al-Salam S, Al-Kayyali BS, Acinic cell carcinoma of the salivary glands: a literature review, Hematol Oncol Stem Cell Ther 2 (2009) 259-64. https://doi.org/10.1016/s1658-3876(09)50035-0.

[46] Park JH, Choi JY, Hong R, Do NY, Clear cell myoepithelial carcinoma in the base of the tongue: Case report and review of the literature, Oncol Lett 4 (2012) 1241-3. https://doi.org/10.3892/ol.2012.900.

[47] Nguyen S, Perron M, Nadeau S, Odashiro AN, Corriveau MN, Epithelial Myoepithelial Carcinoma of the Nasal Cavity: Clinical, Histopathological, and Immunohistochemical Distinction of a Case Report, Int J Surg Pathol 26 (2018) 342-6. https://doi.org/10.1177/1066896917747732.

[48] Habibi A, Saghravanian N, Zare R, Jafarzadeh H, Clear cell variant of extraosseous calcifying epithelial odontogenic tumor: a case report, J Oral Sci 51 (2009) 485-8. https://doi.org/10.2334/josnusd.51.485.

[49] Harada A, Matsumoto S, Yasumizu Y, Shojima K, Akama T, Eguchi H, Kikuchi A, 2021. Localization of KRAS downstream target ARL4C to invasive pseudopods accelerates pancreatic cancer cell invasion. Elife, 10. https://doi.org/10.7554/eLife.66721.

[50] Lo Muzio L, Campisi G, Farina A, Rubini C, Pastore L, Giannone N, Colella G, Leonardi R, Carinci F, Effect of p63 expression on survival in oral squamous cell carcinoma, Cancer Invest 25 (2007) 464-9. https://doi.org/10.1080/07357900701509387.

[51] Hervouet E, Vallette FM, Cartron PF, Impact of the DNA methyltransferases expression on the methylation status of apoptosis-associated genes in glioblastoma multiforme, Cell Death Dis 1 (2010), e8. https://doi.org/ 10.1038/cddis.2009.7

[52] Zhao R, Fallon TR, Saladi SV, Pardo-Saganta A, Villoria J, Mou H, Vinarsky V, Gonzalez-Celeiro M, Nunna N, Hariri LP, Camargo F, Ellisen LW, Rajagopal J, Yap tunes airway epithelial size and architecture by regulating the identity, maintenance, and self-renewal of stem cells, Dev Cell 30 (2014), 151-65. https://doi.org/ 10.1016/j.devcel.2014.06.004

[53] Solar AA, Schmidt BL, Jordan RC, Hyalinizing clear cell carcinoma: case series and comprehensive review of the literature, Cancer 115 (2009) 75-83. https://doi.org/10.1002/cncr.23974.

Figure 1

Click here to access/download;Figure;Figure 1 CCSCC Hasegawa et al rev.tiff

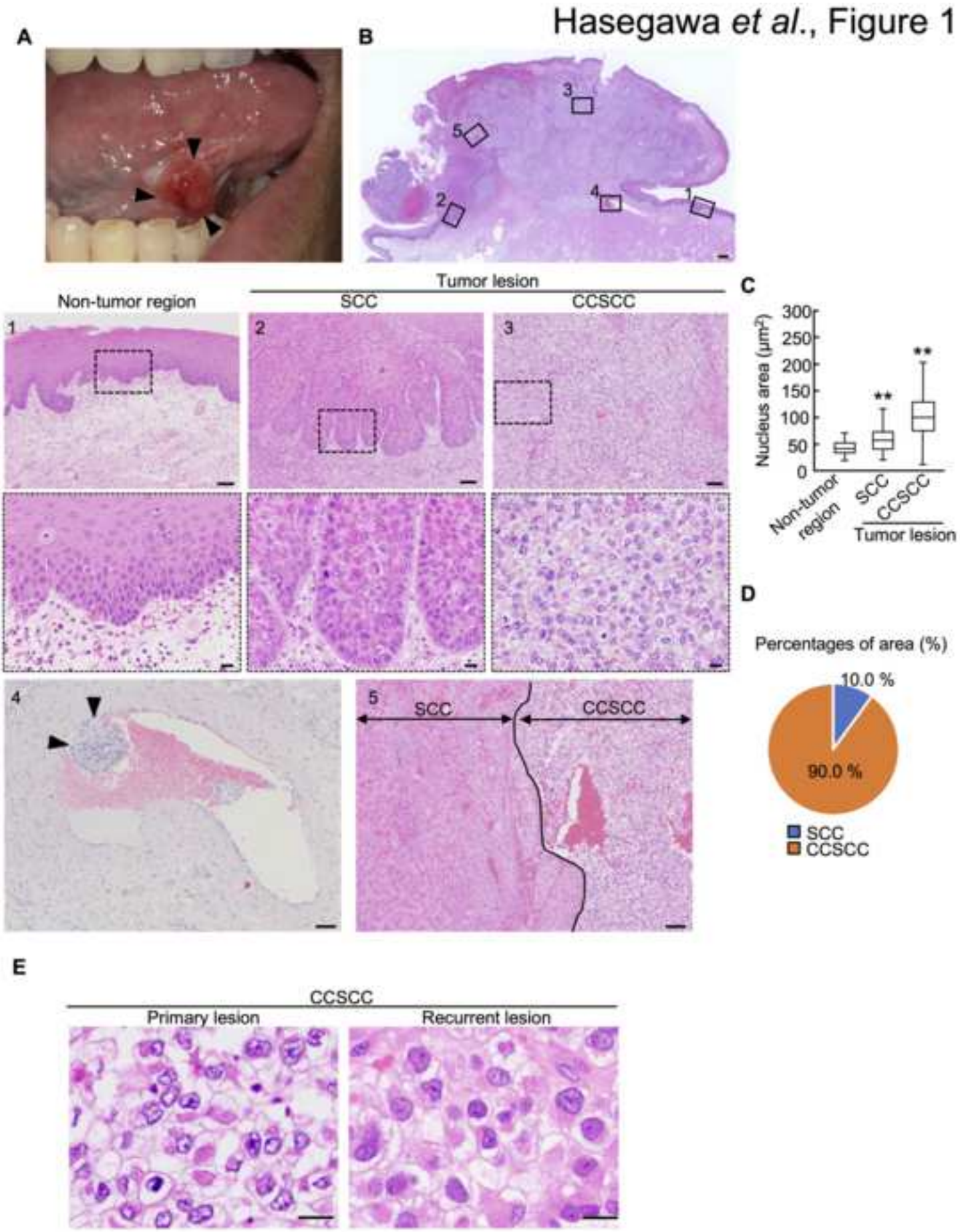

Figure 2

Click here to access/download;Figure;Figure 2 CCSCC Hasegawa et al rev.tiff

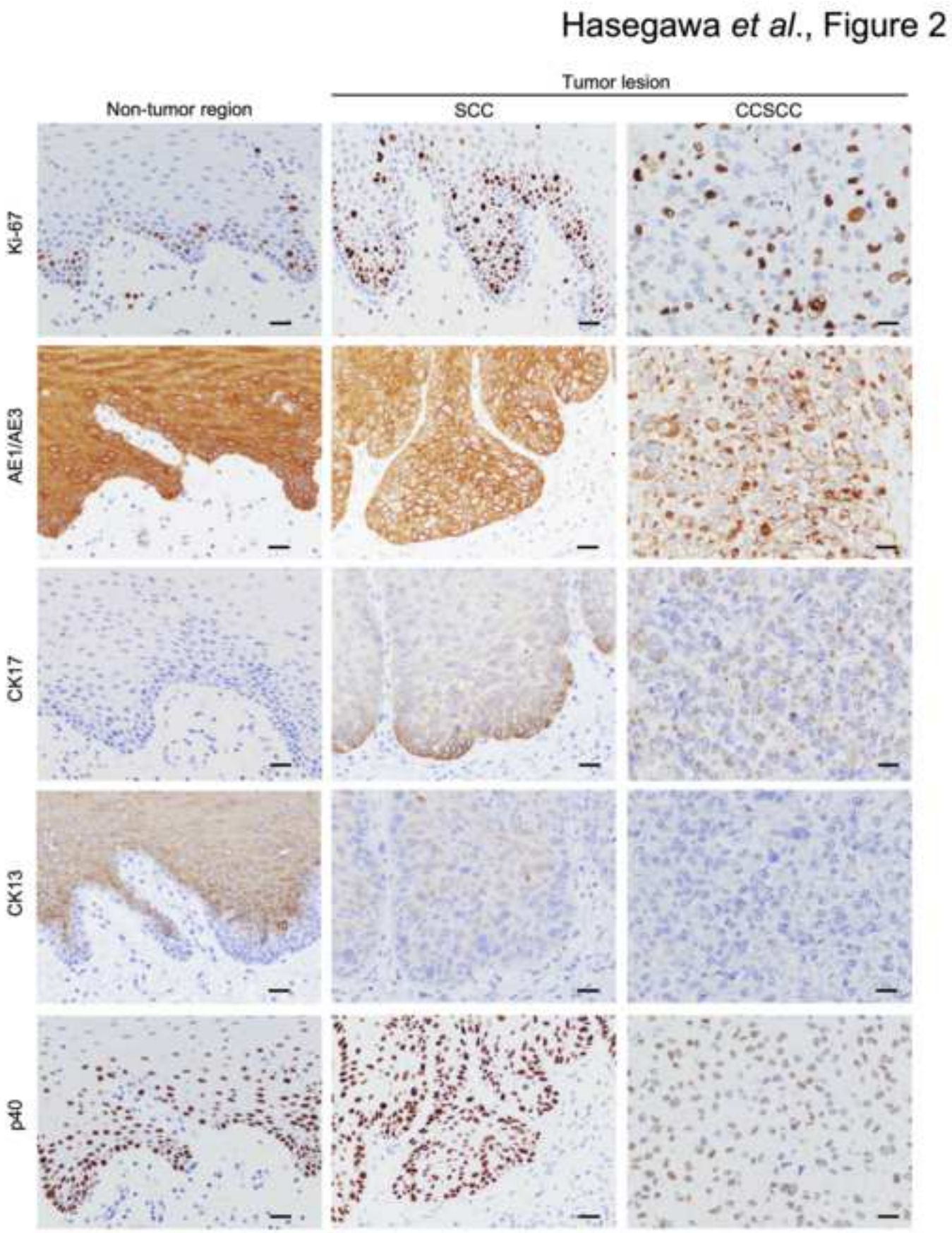

Figure 3

Click here to access/download;Figure;Figure 3 CCSCC Hasegawa et al rev.tiff

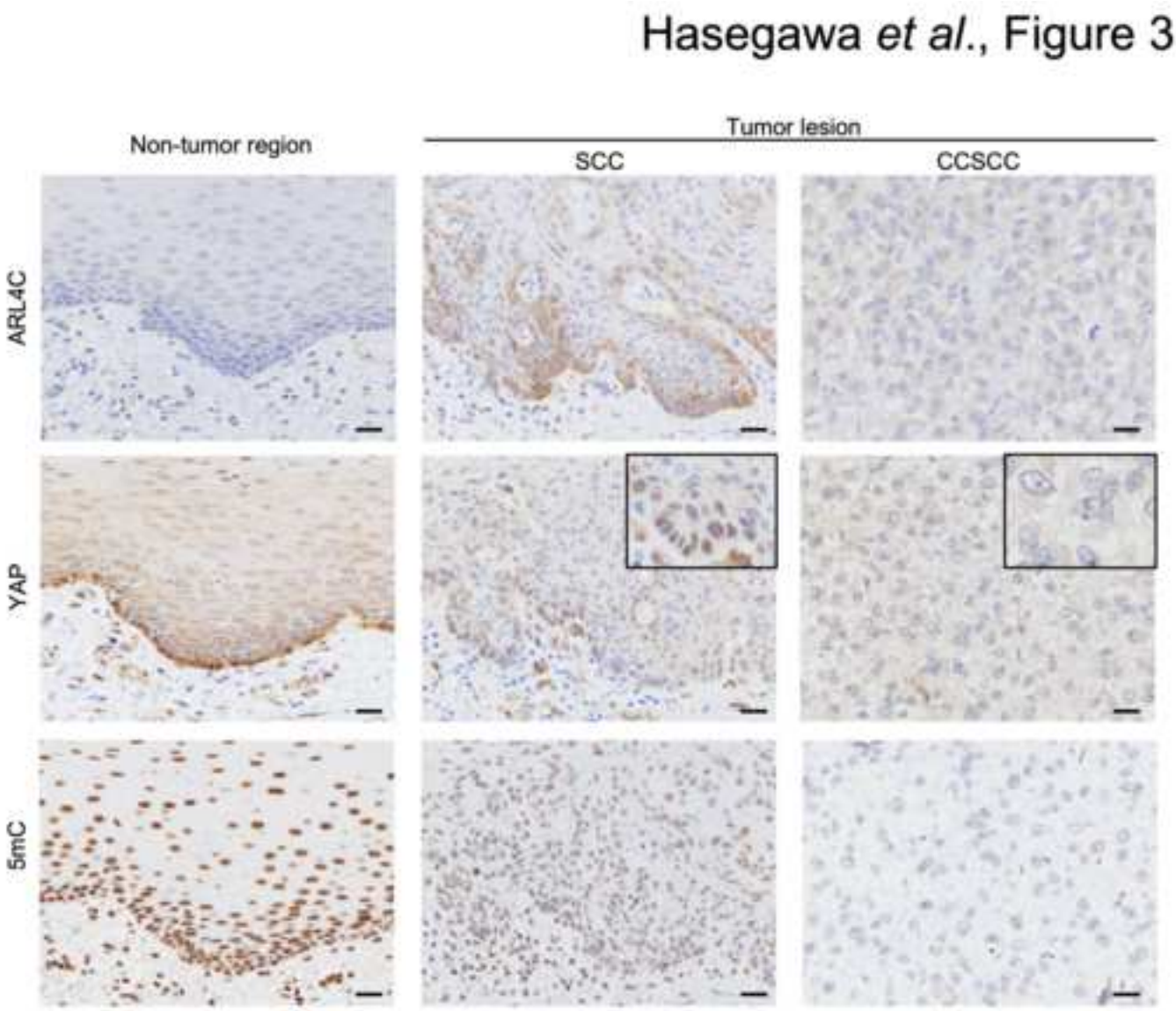

Figure 4

Click here to access/download;Figure;Figure 4 CCSCC Hasegawa et al rev.tiff

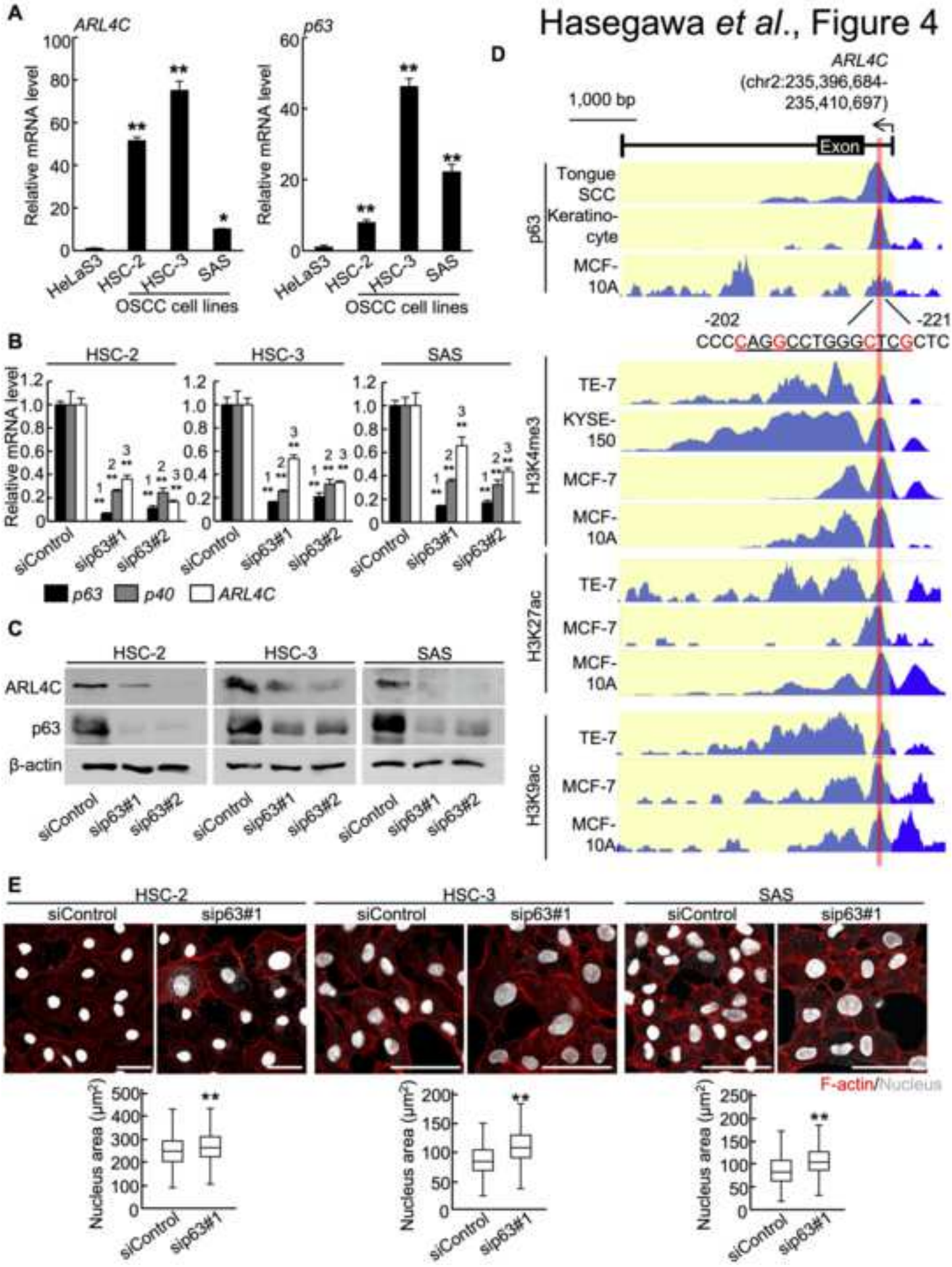

Figure 5

Click here to access/download;Figure;Figure 5 CCSCC Hasegawa et al rev.tiff

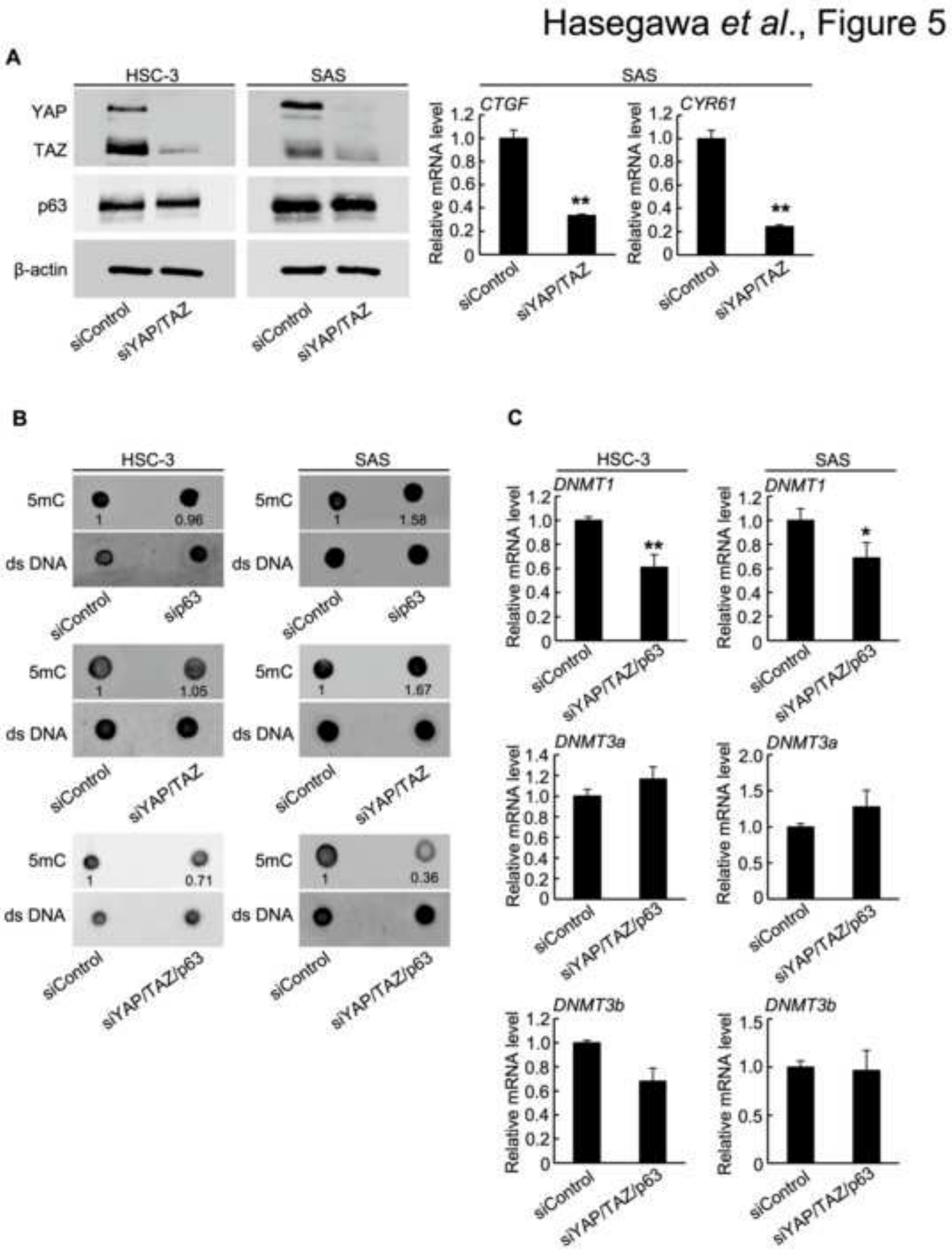

Table 1 A summary of the present case and 6 cases of CCSCC originating from oral cavity.

Case	Author, year	Age/ Sex	Location	Recurrent	Metastasis	Special stains	Immuno histo chemistry
1	Frazier et al. 2012 [8]	59/F	Mandible gingiva	N/A	N/A	PAS (+) Mucicar-mine (-)	
2	Nainani et al. 2014 [9]	52/M	Buccal mucosa	N/A	LN	PAS (-) Mucicar-mine (-)	S-100 (-)
3	Kaliamoorthy et al. 2015 [10]	35/F	Lateral tongue and lingual vestibule	N/A	No	PAS (-) Mucicar-mine (-)	AE1/AE3 (+) SMA (-)
4	Khoury et al. 2017 [11]	66/F	Tongue to the floor of the mouth	N/A	Lung	PAS (+) Mucicar-mine (±)	S-100 (-) SMA (-)
5	Devi et al. 2017 [12]	55/M	Maxillary alveolar ridge	N/A	LN	PAS (-) Mucicar-mine (-)	S-100 (-)
6	Ramani et al. 2021 [13]	42/F	Mandible alveolar mucosa	+	N/A	PAS (-) Mucicar-mine (-)	S-100 (-) SMA (-)
7	Present Case	70/M	Tongue	+	LN, Lung	PAS (-) Mucicar-mine (-)	AE1/AE3 (+) S-100 (-) SMA (-)

F, female; M, male; +, positive; -, negative; N/A, not applicable, LN; cervical lymph node

Conflict of Interest Disclosures: None of the authors have any relevant financial relationship(s) with a commercial interest.

Author contributions

Kana Hasegawa: Investigation, Writing - Original Draft, Funding acquisition.: **Shinsuke Fujii:** Conceptualization, Methodology, Writing - Review & Editing, Funding acquisition.: **Kari J Kurppa:** Supervision.: **Takashi Maehara, Kazunari Oobu, Seiji Nakamura:** Resources.: **Tamotsu Kiyoshima:** Project administration, Writing - Review & Editing, Funding acquisition. All authors were involved in writing the paper and had final approval of the submitted and published versions.

Acknowledgments

The authors thank Dr. M. Sakamoto for searching clinical information in this research, Drs. H. Wada, R. Nagano, M. Kokura and Mr H. Otoba, Ms. M. Egami and Mr. N. Hayama for valuable technical support in this research.